Arabidopsis seedlings display a remarkable resilience under severe mineral starvation using their metabolic plasticity to remain self-sufficient for weeks

Elise Réthoré, Sabine d'Andrea, Abdelilah Benamar, Caroline Cukier, Dimitri Tolleter, Anis M Limami, Marie-Hélène Avelange-Macherel, David Macherel

DR DAVID MACHEREL (Orcid ID : 0000-0002-3352-2185)

Article type : Original Article

Arabidopsis seedlings display a remarkable resilience under severe mineral starvation using their metabolic plasticity to remain self-sufficient for weeks

Elise Réthoré[1], Sabine d'Andrea[2], Abdelilah Benamar[1], Caroline Cukier[1], Dimitri Tolleter[1], Anis M. Limami[1], Marie-Hélène Avelange-Macherel[1], David Macherel[1]*

[1]IRHS, Université d'Angers, INRA, Agrocampus-Ouest, SFR 4207 Quasav, 42 rue Georges Morel, 49071 Beaucouzé, France

[2] Institut Jean-Pierre Bourgin, INRA, AgroParisTech, CNRS, Université Paris-Saclay, RD10, 78026 Versailles, France

***Correspondence:** david.macherel@univ-angers.fr; Tel.: +33-241-225-531

Running head: Seedling prolonged life under mineral starvation

This article has been accepted for publication and undergone full peer review but has not been through the copyediting, typesetting, pagination and proofreading process, which may lead to differences between this version and the Version of Record. Please cite this article as doi: 10.1111/tpj.14325

Key words: Arabidopsis, carbohydrate metabolism, energy metabolism, nutrient limitation, photorespiration, photosynthesis, plastoglobule, respiration, seedling

Abstract

During the life cycle of plants, seedlings are considered vulnerable because they are at the interface between the highly stress tolerant seed embryos and the established plant, and must develop rapidly, often in a challenging environment, with limited access to nutrients and light. Using a simple experimental system, whereby the seedling stage of Arabidopsis is considerably prolonged by nutrient starvation, we analysed the physiology and metabolism of seedlings maintained in such conditions up to four weeks. Although development was arrested at the cotyledon stage, there was no sign of senescence and seedlings remained viable for weeks, yielding normal plants after transplantation. Photosynthetic activity compensated for respiratory carbon losses, and energy dissipation by photorespiration and alternative oxidase appeared important. Photosynthates were essentially stored as organic acids, while the pool of free amino acids remained stable. Seedlings lost the capacity to store lipids in cytosolic lipid droplets, but developed large plastoglobuli. Arabidopsis seedlings arrested in their development because of mineral starvation displayed therefore a remarkable resilience, using their metabolic and physiological plasticity to maintain a steady state for weeks, allowing resumption of development when favourable conditions ensue.

Introduction

Seedlings play a pivotal role in the life cycle of plants, forming the bridge between the heterotrophic embryo and the established photo-autotrophic plant. Emerging from the protective coverings of the seed coat in the soil or on the surface, the seedling is immediately exposed to a range of abiotic and biotic stressors. The success of the seedling establishment is thus critical for the development of plant populations in the natural environment and in the context of crop production (Leck *et al.*, 2008). This is reflected by the importance afforded to the concept of seed vigour, which is the combination of intrinsic seed properties that, besides storage ability, contribute to efficient germination and seedling emergence under unfavourable environmental conditions (Finch-Savage and Bassel, 2016). In spite of its essential role in plant life, there is no consensus definition of what constitutes the seedling

stage, with disparities depending on species and type of study (Hanley *et al.*, 2004). While the start of the seedling stage is unequivocally marked by radicle protrusion, the timing of its end is often less clear. In the case of Arabidopsis (*Arabidopsis thaliana* (L.) Heinh.), the seminal stereologic study of (Mansfield and Briarty, 1996) described the rapid succession of developmental and physiological transitions of Arabidopsis early development. The developmental stages were later phenotypically established throughout the whole life cycle to unify the collection of phenotypic data, although a seedling stage was not clearly assigned (Boyes *et al.*, 2001). Hereafter, we will consider that the seedling stage starts with radicle emergence and terminates with the elongation of the first two leaves, lasting around six days in the conditions of Boyes *et al.* (2001). Arabidopsis, now well recognized for its central role as a genetic model, is a small ruderal weed with a rapid life cycle, which is able to thrive in poor soils and in a great variety of climates (Mitchell-Olds and Schmitt, 2006; Krämer, 2015). Its seeds are minuscule (< 0.5 mm), and the lipid reserves are sufficient only to fuel initial embryo growth, including the rapid development of photosynthetic tissues that is essential for establishment. This transition is part of photomorphogenesis, a developmental program orchestrated by photoreceptors and an array of signalling cascades that, within a few hours, transforms the germinated embryo into a phototrophic seedling (Wu, 2014; Warpeha and Montgomery, 2016). Further growth and development of the seedling appears to be largely dependent on the nutritional status, and in particular upon the C/N balance (Martin *et al.*, 2002; Zheng, 2009). This developmental regulation requires the coordinated expression of clusters of genes in response to nutrient sensing and signalling pathways, including hormones and microRNAs regulators (Liang *et al.*, 2012; Vidal *et al.*, 2014). While the mechanisms of seed storage oil mobilization have been thoroughly investigated (Graham, 2008), the physiology and metabolism of the autotrophic seedling has received less attention, though a recent study revealed a metabolic shift associated with the transition from seed to seedling, which appeared largely under transcriptional control (Silva *et al.*, 2017). Although Arabidopsis cotyledons are embryonic organs, they are partially homologous to leaves since they carry out photosynthesis, and numerous mutants show partial transformation of specific features of one organ onto the other, like for instance, the appearance of leaf trichomes on cotyledons (Chandler, 2008). The role of cotyledons as sources of photosynthesis-derived sugars to control and fuel root growth of Arabidopsis seedlings has been demonstrated, emphasizing the sequential role of light, first as a developmental trigger, then as an energy source (Kircher and Schopfer, 2012). Arabidopsis seedlings are thus pioneer individuals able to perform most of basic plant metabolism, and the importance of their early life for local

adaptation was recently highlighted in a large scale field study (Postma and Ågren, 2016). In the environment, seeds may germinate in conditions where mineral nutrients are very limited, which may compromise subsequent development and seedling establishment. To our knowledge, little is known about how seedlings adapt their metabolism to survive under nutrient starvation until conditions improve. We have previously described a liquid culture system in which the seedling stage can be extended because of nutrient limitation (Benamar *et al.*, 2013). In this system, Arabidopsis seeds are germinated in Evian natural mineral water under shaking, producing seedlings that are photosynthetically active, but unable to form leaves because of the low amount of mineral nutrients available. The initial amount of nutrients present in the mineral water avoids a rapid elongation of the radicle, preventing the clumping of seedlings that would occur in deionised water. Although seedlings are grown in liquid, the medium remains normoxic thanks to the large surface of the wells and shaking. Even though this system is artificial, and it is unlikely that seedlings would be exposed to such a severe mineral deficiency in nature, it offers a useful model to study the seedling stage, which is difficult to investigate because it is transient and accompanied by dramatic changes in development, physiology and metabolism. These "arrested-development" seedlings remain green for several weeks, but it is unclear how they manage to survive under mineral starvation. One hypothesis is that photosynthetic activity is sufficient to compensate for carbon losses via respiration and that macronutrients are recycled, as growth is completely repressed. Here, we present the results of our investigation into the physiology and metabolism of seedlings maintained for up to four weeks under conditions of "arrested-development". Besides providing a comprehensive view of the physiology of seedlings, our results uncovered the importance of energy-dissipation mechanisms to overcome the seemingly most hazardous stage in plant life.

Results

Prolonging early seedling life

When Arabidopsis seedlings are grown in liquid culture in Evian natural mineral water, they are not able to develop true leaves, likely because of nutrient limitation (Benamar *et al.*, 2013). In order to better understand the developmental profile and long-term survival of seedlings in such conditions, we first examined their kinetics of development and growth. Hypocotyl and cotyledon emergence occurred between three and four days post-stratification,

and full opening of cotyledons (Stage 1.0; Boyes *et al*., 2001) was reached after around seven days in our system (Figure 1a), instead of three days post-stratification on half-strength Murashige and Skoog (MS) medium (Boyes *et al.*, 2001). Seedlings then continued to grow (radicle and cotyledon expansion) for approximately seven days, but their development was arrested since true leaves did not appear (Figure 1a). This arrest in development is likely due to the low amounts of nitrate (23 µg/well) and potassium (6 µg/well) and the absence of phosphate in the initial volume of Evian natural mineral water. Fresh weight increased sharply up to around 180 mg per well during the first week, then rather slowly during the three following weeks, with a maximum of around 220 mg per well, reflecting the developmental arrest of seedlings (Figure 1b). Dry weight remained almost constant during the four weeks of culture, which demonstrates that seedling final biomass essentially depends on initial seed mass. Interestingly, while the seedlings remained in a developmental steady state for several weeks, they remained green, without anthocyanin accumulation, and free of necrosis (Figure 1a). Since the medium is almost devoid of mineral nutrients after ten days of culture (Benamar *et al.*, 2013), we checked if seedlings remained fully viable, i.e. able to resume their development after transfer to soil. They were indeed able to produce normal plants on soil, even if they had spent up to four weeks in liquid medium (Supporting Information Figure S1). Only a slight growth retardation was observed for seedlings that stayed two to four weeks in liquid medium, compared to plants directly sown on soil. Combined, these results demonstrate that young seedlings, blocked in their development because of severe nutrient deprivation, can survive in a steady state for weeks, and resume normal development in favourable conditions.

Energy metabolism maintenance under developmental arrest

We hypothesized that maintenance of energy transduction would be essential to allow long term survival of seedlings under mineral nutrient starvation. During the first three days, dark respiration sharply increased up to around 90 nmol $O_2.s^{-1}.g^{-1}$ DW as there was a high energy demand for germination and early growth; then it decreased rapidly from day three until day seven, while seedlings became increasingly photosynthetically active (Figure 1c). Afterwards, the respiratory rate decreased more gradually to stabilize at around 20 nmol $O_2.s^{-1}.g^{-1}$ DW. The maximal net photosynthetic activity (fluence rate 700 µmol photon.$m^{-2}.s^{-1}$) increased sharply between days four and seven, and was then maintained at around 120 nmol $O_2.s^{-1}.g^{-1}$ DW (Figure 1c). These values of net photosynthesis and dark respiration of seedlings, on a dry weight basis, were lower than those of infiltrated four-week-old leaf tissue

(318 ± 35 and 38 ± 4 nmol $O_2.s^{-1}.g^{-1}$ DW, respectively). However, values based on chlorophyll amount were similar between leaf tissue and seedlings (25.4 ± 2.5 and 28.5 ± 1.6 nmol $O_2.s^{-1}.mg^{-1}$ chlorophyll, respectively) because seedlings naturally contain non-green tissues and have thus a lower content of chlorophyll, which could also decrease because of nutrient limitation. Net photosynthesis was also measured with a lower light intensity corresponding to growth room conditions (Figure 1c). It is noticeable that on day four, seedlings photosynthetic activity could already compensate for respiration. On day seven, the rate of net photosynthesis was twice that of dark respiration, and from day 14 to day 28 it was three times higher (Figure 1c). Therefore, after seven days of growth, photosynthetic activity during the day could theoretically compensate for carbon losses due to respiration both in the light and in the dark period (16h / 8h diurnal cycle). We also examined the light response of seven-day-old seedlings, in particular to determine if respiration was inhibited in the light (Figure 2). In many plant species, an inhibition of respiration occurs around the light compensation point, known as the Kok effect (Kok, 1949). While the underlying physiological mechanisms are still debated (Heskel *et al.*, 2013; Tcherkez *et al.*, 2017), we are not aware of any investigation of the Kok effect at the cotyledon stage. To quantify the effect, which is revealed by a typical break in the light response curve, we applied two independent linear regressions for light intensities either below (slope B), or above (slope A) the apparent breakpoint (Figure 2). The lower value of slope A reflects the apparent inhibition of respiration above the compensation point, and the Kok effect was thus estimated using the formula 100x[1-(A/B)]. This analysis was performed on four independent replicates (Supporting Information Table S1). A clear Kok effect was found in both seedlings (19.7 ± 5.8 %) and leaves (45 ± 9.6 %), but it was significantly higher in the latter. This difference could possibly be due to the activity of root respiration in seven-day-old seedlings: dissected roots contributed to 39.2 ± 4.0 % of total dark respiration. Indeed, the light inhibition in photosynthetic tissues could be partially compensated by an increase in root respiration due to increased carbohydrate supply in the light. Correlations between leaf photosynthesis and root respiration have been reported (Noguchi, 2005), but we are not aware of such data for seedlings. Whatever the mechanisms behind the Kok effect, by taking into account the overall inhibition of respiration in the light, values of gross photosynthesis could be extrapolated for seven-day-old seedlings and four-week-old leaf tissues (35.7 and 28.0 nmol $O_2.s^{-1}.mg^{-1}$ chlorophyll, respectively). Collectively, these results suggest that the photosynthetic capacity of chloroplast is comparable in leaf and cotyledon cells.

Considering the role of the alternative oxidase (AOX) pathway in energy dissipation and stress adaptation in plants (McDonald *et al.*, 2002), we sought to estimate its capacity in seedlings. The KCN-resistant oxygen consumption of seedlings was found to be sensitive to the AOX inhibitor propyl-gallate (Benamar *et al.*, 2013), but since maximal inhibition was reached only slowly, we used KCN-resistant respiration as a proxy for AOX capacity, and KCN-sensitive respiration as a proxy for the capacity of the cytochrome oxidase pathway (COX). The COX capacity showed a strong transient increase from imbibition to day three, while AOX capacity remained low, which is in agreement with the requirement for an efficient energy metabolism during germination and early seedling development (Figure 3a). During transition to photo-autotrophy (around day four), there was a marked change since COX capacity decreased while that of AOX increased sharply, and after day seven the AOX capacity remained around three times higher than that of the COX pathway (Figure 3a). This suggests that energy dissipation through the AOX pathway is important for seedlings maintained under mineral starvation. In comparison, in infiltrated four-week-old leaf tissue, the ratio of AOX/COX capacity was much lower (around 0.8) than in seedlings of the same age. AOX protein amounts were indeed higher in seedlings than in leaves (Figure 3b and 3c). However, the doubling of AOX abundance between day 14 and day 21 was not correlated with a corresponding increase in the seedling AOX capacity (Figure 3), suggesting a post-translational regulation. Another way for photosynthetic tissues to dissipate energy is through photorespiration, a pathway found in all oxygenic organisms, but which is highly active in the leaves of C3 plants exposed to stress conditions (Atkin and Macherel, 2009; Maurino and Peterhansel, 2010). We compared, in leaves and in seedlings, the level of GDC-H, a subunit of the mitochondrial glycine decarboxylase complex involved in photorespiration. The amount of GDC-H was as high in seven-day-old seedlings as in mature leaves, and increased during the following weeks of culture (Figure 3b and 3c). Although the presence of other photorespiratory proteins have not been tested, the GDC-H abundance is an indication that seedlings have the capacity to operate photorespiration. To challenge the importance of photorespiration in seedlings, we studied the behaviour of *glyk1-1*, a null mutant for D-glycerate 3-kinase, an enzyme exclusively involved in the last step of the pathway in chloroplasts (Boldt *et al.*, 2005). After one week, the *glyk1-1* mutant started to display a chlorotic phenotype that progressively led to death one week later (Supporting Information Figure S2). This is in fact similar to what happens when *glyk1-1* seeds are germinated on soil in normal air, since seedlings are able to reach the cotyledon stage but then rapidly die (Boldt *et al.*, 2005). We could further confirm that photorespiration was important for survival of

seedlings in our system by supplementing CO_2, which was achieved by continuous perfusion of the medium with 10 mM $NaHCO_3$. In these conditions, *glyk1-1* seedlings remained green for at least two weeks (Supporting Information Figure S2). This strongly suggests that the photorespiratory pathway is essential for seedlings maintained under conditions of mineral nutrient starvation. Taken together, these analyses reveal that seedlings arrested at the cotyledon stage maintain a homeostatic energy balance between efficient photosynthesis, respiration and energy dissipating mechanisms.

Metabolic adaptation to mineral nutrient starvation

Considering the capacity of seedlings to remain alive for weeks in almost pure water, we wondered how their primary metabolism was adjusted under such steady-state conditions. Seedling metabolism was investigated by performing targeted metabolic profiling for amino acids, organic acids, and sugars during the first four weeks of their life. Dry seeds and four-week-old leaves were used for comparison. The abundances of 32 metabolites are indicated in Supporting Information Table S2. One striking results was that the organic/amino acids ratio was much higher in seedlings (e.g. 15x at 28 days) than in dry seeds and leaves (0.8x and 1.4x, respectively) (Figure 4a). Compared to leaves, seedlings had a much larger pool of organic acids and a smaller pool of amino acids. When considering the repartition within the organic acid pool, the major differences between leaves and seedlings were the large decrease in fumarate and increases in malate and oxoglutarate (Figure 4b). In terms of content, this corresponds to a two-fold lower amount of fumarate, and to higher amounts of malate (8x) and oxo-glutarate (30x) for 28 day-old seedlings compared to leaves of the same age (Supporting Information Table S2). The malate accumulation in seedlings is impressive (up to 350 $nmol.mg^{-1}$ DW) since it is comparable to the values found in the day for leaves of the obligate CAM species *Agave americana* (Abraham *et al.*, 2016). Concerning the repartition within the amino acid pool, the major differences between leaves and 28 day-old seedlings were the decreases in Asp, Thr, Ala, Ser and the increase in Gly (Figure 4c). In terms of content, this corresponds to a higher level of Gly (3x) and lower levels of Asp (27x), Thr and Ala (11x), and Ser (6x) (Supporting Information Table S2). Total sugar content was also higher in seedlings than in leaves, especially for glucose and fructose (Supporting Information Table S2). Sucrose was the major sugar in dry seeds, but very low amounts were detected in leaves or seedlings. Stachyose, an abundant oligosaccharide in seeds (approx.

20% of total sugars), was still found in seedlings at all ages, albeit at much lower levels (1-2 %), but was not detected in leaves.

As expected, metabolite content was distinctly different between dry seeds and four day-old seedlings, with the total amount of metabolites 13 times higher in seedlings (Figure 4a). The main modifications in the proportion of organic acids were an increase in malate and oxoglutarate and a decrease in citrate and fumarate (Figure 4b). The proportions of amino acids were markedly different: Glu, Asn and Asp together represented 67 % of amino acids in dry seeds, but only 17 % in four day-old seedlings, in which Gln (30 %) and GABA (15 %) were the most abundant amino acids, the latter being detected at a very low level in seeds (Figure 4c). Between four and 28 days of culture, there was no variation in the total amounts of sugars and amino acids, but an increase in organic acids, which was largely due to the accumulation of malate (2x), oxoglutarate (2x) and fumarate (2.5x), while citrate and succinate contents decreased approximately two-fold (Figure 4; Supporting Information Table S2). Regarding amino acid content, there was an increase in Gly (6 fold), while there was a decrease in Leu (3.5x), Ile (2.5x) and Asn (4x) over the same period. This increase in Gly content and consequently of the Gly/Ser ratio, a marker of photorespiration (Novitskaya *et al.*, 2002), in particular after day 14, supports the idea that photorespiration is taking place in seedlings. Since seedlings were grown under a diurnal light/dark cycle, we compared the metabolic data acquired for midday samples with two other time points: at the end of the light and dark periods, at day seven and day 14. There were few differences between data acquired at different times on the same day, except for a large increase in Gly and Ser at the end of the light period (Supporting Information Figure S3; Supporting Information Table S3), which further agrees with an active photorespiration. As a whole, these analyses highlight the major metabolic changes occurring after germination, and illustrate the metabolic adaptation of seedlings to survival for weeks under severe mineral starvation.

Carbon mobilization and storage during germination and seedling life

Since the DW was stable over the four weeks of culture, but seedlings were fully photosynthetically competent after germination, we investigated the fate of carbon mobilization and storage. Arabidopsis seeds store carbon mainly as triacylglycerols (TAGs) which are deposited in cytosolic lipid droplets (LDs) and used to sustain development of the seedling until autotrophy (Kelly *et al.*, 2011). Although, LDs are consumed rapidly after germination (Siloto *et al.*, 2006; Deruyffelaere *et al.*, 2015), it has also been shown that low

nitrogen can retard the breakdown of lipid reserves in Arabidopsis seedlings (Martin *et al.*, 2002). We therefore performed microscopic observations of LDs using Nile red, a fluorescent probe which stains neutral lipids. Numerous LDs were detected in cotyledons and hypocotyls on days four and seven, but after 14 days, they were rarely observed in either tissue (Figure 5a). To link these observations with storage lipid degradation, we measured fatty acid (FA) content and composition during germination and seedling culture (Figure 5b, 5c, 5d). Total FA amount dropped rapidly during early seedling development, then declined with a lower rate between four and seven days, and remained stable from 14 to 28 days (Figure 5b). All the major FAs displayed a decrease in abundance (Figure 5d). Linolenic acid (C18:3) became the most abundant, representing almost 40 % of the total FA mass in 28 day-old seedlings, while eicosanoic acid (C20:1), a FA specific to seed storage lipids, was reduced to less than 5 % (Figure 5c). This correlated with a decrease in the abundance of several oleosin proteins (OLE1, OLE2 and OLE4), which are structural components of LDs (Supporting Information Figure S4). OLE2 and OLE4 proteins were detected in dry and germinating seeds but no longer after three days of germination, while OLE1 was detected up to four days, consistently with a previous observation showing that the degradation of OLE2 and OLE4 begins during germination, before the post-germinative degradation of OLE1 (Deruyffelaere *et al.*, 2015). The abundance of isocitrate lyase, as well as its activity and that of malate synthase, sharply increased during germination (maximum at day 3), then rapidly declined (Supporting Information Figure S4 & S5), indicating that glyoxylate cycle was active in the early stage of seedling growth, but not later. Taken together, these results show that in our system, seed TAG reserves are mobilized during early seedling growth, as occurs normally during Arabidopsis seedling establishment (Cornah *et al.*, 2004), and that cytosolic LDs did not reappear during long term mineral starvation. Since there was still some C20:1 remaining in the seedlings when most of the seed LDs had disappeared, we wondered whether seedlings could still store TAGs in plastoglobuli (PGs), which are small plastidial LDs which size often increase during senescence and in response to abiotic stress such as drought, high-light and nitrogen limitation (van Wijk and Kessler, 2017). We thus performed a transmission electron microscopy (TEM) analysis of cotyledons to examine chloroplast ultrastructure. Starch granules were rarely observed in chloroplasts, except in four-day-old seedlings where they were very abundant (Figure 6a). This was confirmed by a qualitative starch staining with Lugol (Supporting Information Figure S6). The transient accumulation of starch at day four could possibly buffer the flow of sugars provided by the operation of the glyoxylate cycle, or serve as a temporary store for photosynthates.

Interestingly, PGs were almost systematically detected in plastids from day seven, and their size strongly increased between day 7 and day 28 (Figure 6b, 6c). Surprisingly, when observing LDs by Nile red staining in seedlings (Figure 5a), we did not detect PGs, even when most chloroplasts contained large PGs according to TEM. To clarify this ambiguity, we used a line expressing a fluorescent protein localized in PGs (Vidi *et al.*, 2006). Using 14-day-old seedlings, PGs labelled with GFP were clearly detected in chloroplasts by confocal microscopy, but were not stained by Nile red (Supporting Information Figure S7). This suggests that the dye does not enter chloroplasts, or is not able to stain PG neutral lipids. Collectively, these results highlight the fact that seedlings maintained in nutrient limiting conditions still rely on lipid storage, but with a transition from seed-derived LDs towards PGs.

Discussion

Our results revealed the high resilience of Arabidopsis seedlings: able to survive for at least four weeks with almost no resources other than water and available carbon dioxide, while retaining the ability to develop into normal plants on soil. Under severe mineral starvation, the longevity of seedlings indicates that senescence was not induced, which is surprising because mineral deficiency promotes senescence of leaves or mature plants (Agüera *et al.*, 2010; Balazadeh *et al.*, 2014; Meng *et al.*, 2016). Organ or whole plant senescence indeed often results from a privation of nutrients since resources are allocated to other parts or organs to prioritise growth or reproduction, leading to the concept of exhaustion-death (Molisch, 1938; Thomas, 2002). Repression of senescence in our system could be due to the young developmental stage of the plants since, in young leaves, the induction of senescence is prevented by the expression of the miR164, which negatively regulates ORE1, a master regulator of senescence (Kim *et al.*, 2009; Woo *et al.*, 2013). It is not known whether such a feedback control also occurs in other organs or in whole seedling.

Since the biomass of the photosynthetically active seedlings remained constant, energy dissipation was likely important, as indicated by their high AOX capacity. While oxygen isotope fractionation would be needed to establish the actual partition of electron in the alternative pathway *in vivo*, the AOX capacity is an indicator of the potential electron flux in the pathway (Del-Saz *et al.*, 2018). AOX plays an important role in photosynthetic adaptation to high light (Yoshida *et al.*, 2007; Dinakar *et al.*, 2010) but also to macronutrients limited

conditions (Sieger *et al.*, 2005; Escobar *et al.*, 2006; Vijayraghavan and Soole, 2010). The variations in AOX capacity that we observed were apparently not due to changes in protein abundance according to immunodetection, but could rather result from control by effectors such as keto-acids and the ubiquinone pool reduction state (Millenaar and Lambers, 2003; Vanlerberghe, 2013; Del-Saz *et al.*, 2018).

Leaves also dissipate energy in the light by photorespiration (Bauwe *et al.*, 2010), but whether the pathway is important in the early life of plants, especially in cotyledons of epigean seedlings, has not been thoroughly investigated. In soybean cotyledons, $^{14}CO_2$ incorporation into glycine suggested the occurrence of photorespiration (Marek and Stewart, 1992), and in Arabidopsis, leaf-type peroxisomes accumulating photorespiratory enzymes differentiated during greening of cotyledons (Fukao *et al.*, 2002; Hayashi and Nishimura, 2006). In our system, several evidences support a significant and essential photorespiratory flux in seedlings: abundance of GDC-H, increase in Gly and Ser during the day, death of the *glyk1-1* mutant without CO_2 supplementation. Since the operation of photorespiration has a major effect on cellular redox balance and energy status (Keech *et al.*, 2017), this could be linked to the high capacity of AOX, which could contribute to the reoxidation of NADH produced by GDC (Igamberdiev *et al.*, 1997). In the present study, it is conceivable that, besides other effectors, photorespiratory ammonium also contributed to an increase in AOX capacity (Escobar *et al.*, 2006).

Once seedlings reach their developmental steady-state, carbon is essentially stored as organic acids, in particular malate. Besides its role in the TCA cycle and as carbon store, malate contributes to several metabolic shuttles to control the redox balance and is a key metabolite of the CAM and C4 cycles (Zell *et al.*, 2010; Maurino and Engqvist, 2015). In Arabidopsis leaves, fumarate is expected to be a major transitory sink for photosynthates (Pracharoenwattana *et al.*, 2010), but it accumulated to a much lesser extent in seedlings. Malate storage would allow a rapid mobilization of carbon for seedlings to adapt to the availability of mineral nutrients during establishment in the soil, together with contributing to pH and osmotic regulation. The large accumulation of malate probably results from the lack of a competitive nitrogen metabolism operating as a sink for carbon skeletons used for amino acids or protein synthesis. In agreement with the study of Silva *et al.* (2017), the content of amino acids increased almost three times during germination and early seedling growth. However, it remained fairly constant afterwards, which suggests that, after protein reserve mobilization, nitrogen metabolism essentially consists of the production and recycling of photorespiratory ammonium, without a net gain of nitrogen. The Gly content likely increased

at the expense of other amino acids, in particular Asn. The Asp pathway which starts by the amination of oxaloacetate did not constitute a sink for C skeletons, which is consistent with the accumulation of malate. The low activity of the Asp pathway might be due to the sequestration of the amino donor Gln in the glutamine synthetase/glutamate oxoglutarate amino transferase cycle.

While the developing Arabidopsis embryo stores lipids in cytosolic LDs, seedlings in the steady state were found to display large PGs, a feature reminiscent of leaves subjected to nitrogen limitation, high light stress, or undergoing senescence (van Wijk and Kessler, 2017). To our knowledge, PG accumulation in seedlings has not been documented yet, but in our conditions, the lack of nitrogen likely explains their accumulation. Although their functions are still debated, PGs clearly contribute to the metabolic plasticity of thylakoids through lipid storage and metabolism, especially upon stress relief (van Wijk and Kessler, 2017). High C/N was earlier demonstrated to slow down lipid reserves breakdown in Arabidopsis (Martin *et al.*, 2002), while another study suggested an increase in TAG accumulation in LDs occurred in similar conditions (Yang *et al.*, 2011). In our model, seedlings slowly degraded seed storage lipids, as they still retained 11% of the initial eicosanoic acid (C20:1) content after one week of culture, and lipid storage shifted from cytosolic LDs in dry seeds to PGs in starved seedlings.

The overall results highlight the capacity of Arabidopsis seedlings arrested in their development to survive under severe mineral starvation, by entering into a stationary metabolic state (Figure 7). In some way, this is analogous to the case of microorganisms entering a stationary phase when lacking nutrients, which also display a decrease in metabolic rates (Chubukov and Sauer, 2014). Although we did not measure CO_2 exchange, both the stability of seedling mass and the oxygraphic data support the hypothesis that photosynthetic carbon assimilation compensates for day and night carbon losses. In the illuminated seedlings, mitochondrial CO_2 production originate mostly from glycine breakdown, since the overall activity of the TCA cycle, and thus of respiratory CO_2 release, is expected to decrease because of the inactivation of pyruvate dehydrogenase, especially under photorespiratory conditions (Noguchi and Yoshida, 2008). However, the scene might be more complex since there is strong evidence for the operation of non-cyclic modes of the TCA cycle in different physiological conditions (Sweetlove *et al*., 2010). Under the prevailing low CO_2 conditions in the medium, it is tempting to postulate that CO_2 released in mitochondria could be re-assimilated in the chloroplast (Figure 7). This could likely occur by diffusion (CO_2 easily cross membranes), or through an active mitochondrial bicarbonate export system together

with an organic acid shuttle from the cytosol to the plastid (Zabaleta *et al.*, 2012), since the chloroplast envelope is not permeable to bicarbonate (Tolleter *et al.*, 2017). Ammonia, which is released in large amounts during photorespiration in mitochondria, is expected to be shuttled back and re-assimilated in the plastid (Linka and Weber, 2005). In the context of the nitrogen-starved seedlings, a loss of ammonia would be unsustainable, and therefore nitrogen cycling should operate with high efficiency. Finally, since seedlings growth is restricted, the energy demand is low, essentially devoted to maintenance processes, and is therefore easily supplied by mitochondrial respiration. The high capacity of AOX pathway should contribute to energy dissipation, but also to allow the maintenance of mitochondrial carbon metabolism under low energy demand.

The resilience of seedlings likely contributes to their competitiveness in the environment, and therefore to plant fitness, especially for species with small seeds like Arabidopsis. A major question arising from this study is why seedlings should finally die. Although the experiment was limited to four weeks, seedlings remained green and apparently healthy for longer. Seedlings are apparently in equilibrium, but will inevitably suffer from internal damage because of the myriads of reactions occurring in all cellular compartments, including the necessary turnover of most of cellular components. Indeed, protein quality control and cellular autophagy mechanisms play a major role to counteract cellular aging in most organisms, including plants (Lionaki and Tavernarakis, 2013; Üstün *et al.*, 2017; Broda *et al.*, 2018). There is also a strong link between oxidative stress and ageing in animals, and mitochondria have a central role in senescence (Theurey and Pizzo, 2018). Paradoxically, mitochondrial inefficiency appears as a key to longevity, in particular through mild uncoupling, that would prevent oxidative stress by decreasing the proton gradient, thus preventing formation of reactive oxygen species (ROS) (Brand, 2000). In seedlings, mitochondria, but also chloroplasts and peroxisomes are major sources of ROS, and progressive accumulation of oxidative damages could lead to oxidative imbalance, ultimately leading to death. The high capacity of AOX in seedlings should efficiently prevent mitochondrial ROS production, and possibly contribute to their prolonged life under mineral starvation.

To conclude, besides revealing the metabolic plasticity underlying the resilience of seedlings under mineral starvation, this experimental system model will be invaluable not only to study molecular mechanisms that determine lifespan, but also to examine the impact of various abiotic stressors in a stable system independent of growth and development.

Experimental procedures

Plant material

Arabidopsis thaliana Col-0 dry seeds were added to the wells of six-well plates containing 6 mL of commercially available Evian natural mineral water (pH= 7.2; concentration in $mg.L^{-1}$: Ca^{2+}: 80; Mg^{2+}: 26; Na^{+}: 6.5; $K^{+:}$ 1; SiO_2: 15; HCO_3: 360; SO_4^{-}: 12.6; Cl^{-}: 6.8; NO_3^{-}: 3.7), according to Benamar et al. (2013). Plates were incubated at 4°C in the dark for 24 h and then incubated in a growth room (16 h of light, 150 µmol $photons.m^{-2}.s^{-1}$, 21°C/19°C, 60 % humidity) under rotary shaking (135 rpm). Arabidopsis plants were grown on soil under the same growth room conditions. Some experiments were also performed using the photorespiratory mutant *glyk1-1* (Boldt *et al.*, 2005) and a line (35S:PGL35:GFP) expressing a GFP-tagged plastoglobule protein (Vidi *et al.*, 2006). For CO_2 enrichment experiments, after three days of culture the medium was changed for a solution of 10 mM $NaHCO_3$, 10 mM MOPS (pH 7.2) in 25% (v/v) Evian natural mineral water, which was then continuously renewed (around 3 mL per hour).

Biomass measurements

Fresh weight was measured after collecting the content of each well (seeds/seedlings) by filtration with a 0.45 µm nylon membrane (Merck KGaA, Darmstadt, Germany) using a water-driven vacuum pump aspirator. Dry weight was measured after drying the same samples for 24 h at 96°C.

Oxygen measurements

Measurements of O_2 exchange were performed using an Oxylab electrode system with a white light source LED1/W (Hansatech, King's Lynn, UK) at 25°C, in 1 mL Evian natural mineral water containing around 20 mg germinating seeds, 50 mg seedlings or vacuum-infiltrated fragments of mature leaves from four-week-old plants. For net photosynthesis assay, light was calibrated at 150 (growth room conditions) or 700 µmol $photons.m^{-2}.s^{-1}$ (saturating light) using a QRT1 Quantitherm (Hansatech). For light response assay, different light intensities (from 0 to 100 µmol $photons.m^{-2}.s^{-1}$) were applied. Rates were standardized using dry weight or chlorophyll amount. Total chlorophyll was extracted in 1 mL dimethyl-

N-formamide overnight in the dark and total chlorophyll amount was determined by spectrophotometry according to the formula (Total chlorophyll (µg) = 7.04 A664 + 20.27 A647) of Moran (1982), using a microplate reader FLUOstar Omega (BMG Labtech, Ortenberg, Germany).

Western blot

For the immunodetection of glycine decarboxylase H protein (GDC-H), alternative oxidase (AOX1 and AOX2 isoforms) and isocitrate lyase (ICL), total proteins were extracted in 50 mM $NaPO_4$ pH 8, 10 mM Ethylenediaminetetraacetic acid (EDTA), 0.1 % (v/v) Triton-X 100, 0.1 % (m/v) Sarcosyl, 10 mM dithiothreitol (DTT), 1 mM phenylmethane sulfonyl fluoride (PMSF) and antiproteases (cOmplete EDTA-free, Roche, Basel, Switzerland). Protein concentration was determined using the Bradford protein assay (Bio-rad, Marnes-La-Coquette, France) with bovine serum albumin (BSA) as protein standard. Proteins separated on 12 % Stain Free Gels (Bio-Rad) were blotted to PVDF (Merck KGaA, Darmstadt, Germany) using tank transfer (10 mM N-cyclohexyl-3-aminopropane sulfonic acid (CAPS) pH 11, 10 % EtOH). Blots were blocked in TBST buffer (50 mM Tris–HCl, pH 7.4, 150 mM NaCl, 0.1 % (v/v) Tween 20) containing 3 % (m/v) defatted dry milk, then incubated in the same buffer containing primary antibodies for 1.5 h, at 4°C, under shaking. Anti-GDC-H (Cat# AS05074, RRID:AB_1031689), anti-AOX1/2 (Cat# AS04054, RRID:AB_1031839) and anti-ICL (Cat# AS09500, RRID:AB_1832014) rabbit polyclonal antibodies from Agrisera (Vännäs, Sweden) were respectively diluted to 1:3000, 1:1000 and 1:1000 and secondary antibody (goat anti-rabbit IgG horse radish peroxidase conjugated (Cat# AS09602, RRID:AB_1966902), Agrisera) diluted to 1:75,000. Blots were developed with Western Clarity ECL (Bio-Rad). Oleosin immunodetection was performed according to D'Andréa et al. (2007). Protein loading on membrane was estimated by UV detection according to Stain-free technology (Bio-Rad). For semi-quantitative analysis, pixels of chemiluminescence were quantified in every lane and were normalized based on the intensity of the RbcL band detected by UV on the membranes. For each protein, the normalized intensities were then expressed as the percentage of the signal detected in d28 sample on the same membrane.

Metabolic profiling

Seedlings or leaves were harvested and flash frozen using liquid N_2, lyophilized and ground with glass beads (3 mm) using a TissueLyser (Qiagen, Hilden, Germany) at 30 Hz for 1 min. Dry seed samples were ground using a mortar and pestle. Polar metabolites were extracted with 300 µL methanol/750 µL chloroform/300 µL water. Alpha-aminobutyric acid, adipate and melezitose were used as internal standards. Polar phase was dried using a miVac QUATTRO concentrator (SP Scientific, Ipswich, UK) and residue solubilized in 300 µL deionized water. Standardized volumes of samples were dried and derivatized with 50 µL pyridine/methoxyamine hydrochloride (20 mg. mL^{-1}) for 1.5 h at 30°C and then with 50 µL N-Methyl-N-tert-butyldimethylsilyltrifluoroacetamide (MTBSTFA) for 30 min at 70°C. Analyses were carried out according to Bobille et al. (2016), except for the elution profile: 70°C for 5 min, linear gradient of 5°C min^{-1} to 300°C, 300°C for 5 min, resulting in a total run time of 56 min. For the detection of sugars, samples were diluted 1:80 and analysed by HPLC at 30°C with 10 % (m/v) NaOH on a Carbopac PA-1 column (Dionex Corp., Sunnyvale, CA, USA) using pulsed amperometric detection, as described by Tetteroo et al. (1994). Fatty acid analysis of lyophilized samples was performed according to Deruyffelaere *et al*. (2015). All metabolic data were normalized to dry weight measured after lyophilisation.

Optical and transmission electron microscopy

For starch detection, seedlings were depigmented with 96° ethanol overnight at 4°C and stained with Lugol's iodine solution. Observations were performed using an Axio Imager Z2 with an EC Plan-Neofluar 10x objective (Carl Zeiss Microscopy GmbH, Göttingen, Germany). For the observation of lipid droplets, seedlings were incubated for 15 min in Nile red (1 µg.mL^{-1}). Live cell confocal laser scanning microscopy was performed using a Nikon A1 microscope driven by NIS Elements software (Nikon France S.A, Champigny sur Marne, France) with a Nikon Plan Fluor 10x objective (NA 0.3) or a Nikon CFI Apo 40x WI objective (NA 1.25). Excitation/emission wavelengths (nm) were as follows: Nile red, 561/570-620; chlorophyll autofluorescence 638/662-737; GFP 488/500-550. For transmission electron microscopy, samples were fixed in 2.5 % (w/v) paraformaldehyde and 2.5 % (v/v) glutaraldehyde in 50 mM phosphate buffer (pH 7.2) overnight at 4°C under vacuum and post-fixed for 1 h in 1 % (w/v) osmium tetroxide. After dehydration with ethanol they were embedded in epon resin, and ultrathin sections (60 nm) were cut with a diamond knife using a

Leica UC7 (Leica, Rueil Malmaison, France), stained with 3 % (m/v) uranyle acetate in 50° ethanol for 15 min and observed using a JEM 1400 electron microscope (JEOL, Tokyo, Japan). Plastoglobule size was measured by image analysis using Fiji software (Schindelin *et al.*, 2012).

Enzyme assays

Samples of dry seeds or seedlings were ground in liquid nitrogen using a mortar and pestle and proteins were extracted in 50 mM 3-(N-morpholino)propane sulfonic acid (MOPS) pH 7.2, 1 mM EDTA. After centrifugation at 15,000 g for 15 min at 4°C, the supernatant was used for enzymatic assays. Malate synthase and isocitrate lyase assays were adapted from Cooper & Beevers (1969). Malate synthase was measured at 25°C in 50 mM tricine pH 8.0, 5 mM $MgCl_2$, 1.5 mM DTNB (5,5'-dithio-bis-[2-nitrobenzoic acid]), 200 µM acetyl-CoA. The reaction was initiated with 20 mM glyoxylate and absorbance followed at 412 nm with a SPECTROstar Nano (BMG Labtech, Ortenberg, Germany). Isocitrate lyase assay was measured at 25°C in 50 mM MOPS pH 7.2, 5 mM $MgCl_2$, 5 mM DTT, 10 mM phenylhydrazine. Isocitrate (5 mM) was added to start the reaction and absorbance followed at 324 nm.

Statistical analyses

After checking normality and homoscedasticity of variables, Student's test or ANOVA followed by either Tukey's or Dunnett's test were performed on data with $p<0.05$ using SigmaPlot v11.0 (Systat Software Inc., Chicago, IL, USA).

Data statement

All soluble metabolite amounts are available in the supplementary information tables. Raw data for these assays and other experiments (fatty acids, oxygraphy, western blots, microscopy, enzyme assays) are available on request from the corresponding author (david.macherel@univ-angers.fr).

Acknowledgements

We are thankful to Fabienne Simonneau and Aurélia Rolland (IMAC-QUASAV, confocal microscopy), Guillaume Mabilleau and Florence Manero (SCIAM, electron microscopy), Pascale Satour (IRHS-SMS, sugar analysis). We are grateful to Hermann Bauwe (University of Rostock) and Felix Kessler (University of Neuchâtel) for kindly providing the *glyk1-1* and 35S:PGL35:GFP lines. We thank David C. Logan for invaluable suggestions and proofreading of the manuscript. This research was conducted in the framework of the regional programme "Objectif Végétal, Research, Education and Innovation in Pays de la Loire", supported by the French Region Pays de la Loire, Angers Loire Métropole and the European Regional Development Fund.

Conflict of Interests

The authors declare no conflict of interests.

Short Supporting Information Legends

Figure S1. Development of plants after initial culture of seedlings under mineral starvation.

Figure S2. Importance of photorespiration for survival of seedlings under nutrient limitation.

Figure S3. Daily evolution of glycine and serine content in seedlings.

Figure S4. Immunoblot analyses of oleosins (OLE1, OLE2 and OLE4) and isocitrate lyase content in dry seeds (DS) and during germination and seedling culture (up to 28 days).

Figure S5. Activities of glyoxylic cycle enzymes in liquid culture.

Figure S6. Lugol staining reveals the presence of starch on day four but not afterwards

Figure S7. Nile red stains lipid droplets but not plastoglobuli.

Table S1. Estimation of Kok effect in seven-day-old seedlings and mature leaves.

Table S2. Amino acids, organic acids and sugars contents of mature leaves, dry seeds or liquid-grown seedlings.

Table S3. Amino acids, organic acids and sugar contents of liquid-grown seedlings during daytime

References

Abraham, P.E., Yin, H., Borland, A.M., et al. (2016) Transcript, protein and metabolite temporal dynamics in the CAM plant Agave. *Nat. Plants*, **2**, 1–10.

Agüera, E., Cabello, P. and la Haba, P. de (2010) Induction of leaf senescence by low nitrogen nutrition in sunflower (*Helianthus annuus*) plants. *Physiol. Plant.*, **138**, 256–267.

Atkin, O.K. and Macherel, D. (2009) The crucial role of plant mitochondria in orchestrating drought tolerance. *Ann. Bot.*, **103**, 581–597.

Balazadeh, S., Schildhauer, J., Araújo, W.L., Munné-Bosch, S., Fernie, A.R., Proost, S., Humbeck, K. and Mueller-Roeber, B. (2014) Reversal of senescence by N resupply to N-starved *Arabidopsis thaliana*: Transcriptomic and metabolomic consequences. *J. Exp. Bot.*, **65**, 3975–3992.

Bauwe, H., Hagemann, M. and Fernie, A.R. (2010) Photorespiration: players, partners and origin. *Trends Plant Sci.*, **15**, 330–336.

Benamar, A., Pierart, A., Baecker, V., Avelange-Macherel, M.H., Rolland, A., Gaudichon, S., Gioia, L. di and Macherel, D. (2013) Simple system using natural mineral water for high-throughput phenotyping of *Arabidopsis thaliana* seedlings in liquid culture. *Int. J. High Throughput Screen.*, **4**, 1–15.

Bobille, H., Limami, A.M., Robins, R.J., Cukier, C., Floch, G. Le and Fustec, J. (2016) Evolution of the amino acid fingerprint in the unsterilized rhizosphere of a legume in relation to plant maturity. *Soil Biol. Biochem.*, **101**, 226–236.

Boldt, R., Edner, C., Kolukisaoglu, U., Hagemann, M., Weckwerth, W., Wienkoop, S., Morgenthal, K. and Bauwe, H. (2005) D-GLYCERATE 3-KINASE, the last unknown enzyme in the photorespiratory cycle in Arabidopsis, belongs to a novel kinase family. *Plant Cell*, **17**, 2413–20.

Boyes, D.C., Zayed, A.M., Ascenzi, R., McCaskill, A.J., Hoffman, N.E., Davis, K.R. and Gorlach, J. (2001) Growth stage-based phenotypic analysis of Arabidopsis: A model for high throughput functional genomics in plants. *Plant Cell*, **13**, 1499–1510.

Brand, M.D. (2000) Uncoupling to survive? The role of mitochondrial inefficiency in ageing. *Exp. Gerontol.*, **35**, 811–820.

Broda, M., Millar, A.H. and Aken, O. Van (2018) Mitophagy: a mechanism for plant growth and survival. *Trends Plant Sci.*, **23**, 434–450.

Chandler, J.W. (2008) Cotyledon organogenesis. *J. Exp. Bot.*, **59**, 2917–2931.

Chubukov, V. and Sauer, U. (2014) Environmental dependence of stationary-phase metabolism in *Bacillus subtilis* and *Escherichia coli*. *Appl. Environ. Microbiol.*, **80**, 2901–2909.

Cooper, T.G. and Beevers, H. (1969) Mitochondria and glyoxysomes from castor bean endosperm. *J. Biol. Chem.*, **244**, 3507–3513.

Cornah, J.E., Germain, V., Ward, J.L., Beale, M.H. and Smith, S.M. (2004) Lipid utilization, gluconeogenesis, and seedling growth in Arabidopsis mutants lacking the glyoxylate cycle enzyme malate synthase. *J. Biol. Chem.*, **279**, 42916–42923.

D'Andréa, S., Jolivet, P., Boulard, C., Larré, C., Froissard, M. and Chardot, T. (2007) Selective one-step extraction of *Arabidopsis thaliana* seed oleosins using organic solvents. *J. Agric. Food Chem.*, **55**, 10008–10015.

Del-Saz, N.F., Ribas-Carbo, M., McDonald, A.E., Lambers, H., Fernie, A.R. and Florez-Sarasa, I. (2018) An *in vivo* perspective of the role(s) of the alternative oxidase pathway. *Trends Plant Sci.*, **23**, 206–219.

Deruyffelaere, C., Bouchez, I., Morin, H., Guillot, A., Miquel, M., Froissard, M., Chardot, T. and D'Andrea, S. (2015) Ubiquitin-mediated proteasomal degradation of oleosins is involved in oil body mobilization during post-germinative seedling growth in Arabidopsis. *Plant Cell Physiol.*, **56**, 1374–1387.

Dinakar, C., Raghavendra, A.S. and Padmasree, K. (2010) Importance of AOX pathway in optimizing photosynthesis under high light stress: Role of pyruvate and malate in activating AOX. *Physiol. Plant.*, **139**, 13–26.

Escobar, M.A., Geisler, D.A. and Rasmusson, A.G. (2006) Reorganization of the alternative pathways of the Arabidopsis respiratory chain by nitrogen supply: opposing effects of ammonium and nitrate. *Plant J.*, **45**, 775–788.

Finch-Savage, W.E. and Bassel, G.W. (2016) Seed vigour and crop establishment: Extending performance beyond adaptation. *J. Exp. Bot.*, **67**, 567–591.

Fukao, Y., Hayashi, M. and Nishimura, M. (2002) Proteomic analysis of leaf peroxisomal proteins in greening cotyledons of *Arabidopsis thaliana*. *Plant Cell Physiol.*, **43**, 689–696.

Graham, I.A. (2008) Seed storage oil mobilization. *Annu. Rev. Plant Biol.*, **59**, 115–142.

Hanley, M.E., Fenner, M., Whibley, H. and Darvill, B. (2004) Early plant growth: Identifying the end point of the seedling phase. *New Phytol.*, **163**, 61–66.

Hayashi, M. and Nishimura, M. (2006) *Arabidopsis thaliana* - A model organism to study plant peroxisomes. *Biochim. Biophys. Acta - Mol. Cell Res.*, **1763**, 1382–1391.

Heskel, M.A., Atkin, O.K., Turnbull, M.H. and Griffin, K.L. (2013) Bringing the Kok effect to light: A review on the integration of daytime respiration and net ecosystem exchange. *Ecosphere*, **4**, 1–14.

Igamberdiev, A.U., Bykova, N. V. and Gardeström, P. (1997) Involvement of cyanide-resistant and rotenone-insensitive pathways of mitochondrial electron transport during oxidation of glycine in higher plants. *FEBS Lett.*, **412**, 265–269.

Keech, O., Gardeström, P., Kleczkowski, L.A. and Rouhier, N. (2017) The redox control of photorespiration : from biochemical and physiological aspects to biotechnological considerations. *Plant. Cell Environ.*, **40**, 553–569.

Kelly, A.A., Quettier, A.-L., Shaw, E. and Eastmond, P.J. (2011) Seed storage oil mobilization is important but not essential for germination or seedling establishment in Arabidopsis. *Plant Physiol.*, **157**, 866–875.

Kim, J.H., Woo, H.R., Kim, J., Lim, P.O., Lee, I.C., Choi, S.H., Hwang, D. and Nam, H.G. (2009) Trifurcate feed-forward regulation of age-dependent cell death involving miR164 in Arabidopsis. *Science*, **323**, 1053–1058.

Kircher, S. and Schopfer, P. (2012) Photosynthetic sucrose acts as cotyledon-derived long-distance signal to control root growth during early seedling development in Arabidopsis. *Proc. Natl. Acad. Sci.*, **109**, 11217–11221.

Kok, B. (1949) On the interrelation of respiration and photosynthesis in green plants. *Biochim. Biophys. Acta*, **3**, 625–631.

Krämer, U. (2015) Planting molecular functions in an ecological context with *Arabidopsis thaliana*. *Elife*, **4**, 1–13.

Leck, M.A.., Simpson, R.L.. and Thomas, V. (2008) Why seedlings? In M. Parker, V. Thomas; Simpson, Robert L.; Alessio Leck, ed. *Seedling Ecology and Evolution*. Cambridge: Cambridge University Press, pp. 3–13.

Liang, G., He, H. and Yu, D. (2012) Identification of nitrogen starvation-responsive microRNAs in *Arabidopsis thaliana*. *PLoS One*, **7**, e48951.

Linka, M. and Weber, A.P.M. (2005) Shuffling ammonia between mitochondria and plastids during photorespiration. *Trends Plant Sci.*, 10, 461–465.

Lionaki, E. and Tavernarakis, N. (2013) Oxidative stress and mitochondrial protein quality control in aging. *J. Proteomics*, **92**, 181–194.

Mansfield, S.G. and Briarty, L.G. (1996) The dynamics of seedling and cotyledon cell development in *Arabidopsis thaliana* during reserve mobilization. *Int. J. Plant Sci.*, **157**, 280–294.

Marek, L.F. and Stewart, C.R. (1992) Photosynthesis and photorespiration in presenescent, senescent, and rejuvenated soybean cotyledons. *Plant Physiol.*, **98**, 694–699.

Martin, T., Oswald, O. and Graham, I.A. (2002) Arabidopsis seedling growth, storage

lipid mobilization, and photosynthetic gene expression are regulated by carbon: nitrogen availability. *Plant Physiol.*, **128**, 472–481.

Maurino, V.G. and Engqvist, M.K.M. (2015) 2-hydroxy acids in plant metabolism. *Arab. B.*, **13**, e0182.

Maurino, V.G. and Peterhansel, C. (2010) Photorespiration: current status and approaches for metabolic engineering. *Curr. Opin. Plant Biol.*, **13**, 248–255.

McDonald, A.E., Sieger, S.M. and Vanlerberghe, G.C. (2002) Methods and approaches to study plant mitochondrial alternative oxidase. *Physiol. Plant.*, **116**, 135–143.

Meng, S., Peng, J.S., He, Y.N., Zhang, G. Bin, Yi, H.Y., Fu, Y.L. and Gong, J.M. (2016) Arabidopsis NRT1.5 mediates the suppression of nitrate starvation-induced leaf senescence by modulating foliar potassium level. *Mol. Plant*, **9**, 461–470.

Millenaar, F.F. and Lambers, H. (2003) The alternative oxidase: in vivo regulation and function. *Plant Biol.*, **5**, 2–15.

Mitchell-Olds, T. and Schmitt, J. (2006) Genetic mechanisms and evolutionary significance of natural variation in Arabidopsis. *Nature*, **441**, 947–952.

Molisch, H. (1938) *The longevity of plants*, Science Press, Lancaster, pp.124-143.

Moran, R. (1982) Formulae for determination of chlorophyllous pigments extracted with N,N-dimethylformamide. *Plant Physiol.*, **69**, 1376–1381.

Noguchi, K. (2005) Effects of light intensity and carbohydrate status on leaf and root respiration. In H. Lambers and M. Ribas-Carbo, eds. *Plant Respiration: From Cell to Ecosystem*. Dordrecht: Springer Netherlands, pp. 63–83.

Noguchi, K. and Yoshida, K. (2008) Interaction between photosynthesis and respiration in illuminated leaves. *Mitochondrion*, **8**, 87–99.

Novitskaya, L., Trevanion, S.J., Driscoll, S., Foyer, C.H. and Noctor, G. (2002) How does photorespiration modulate leaf amino acid contents? A dual approach through modelling and metabolite analysis. *Plant, Cell Environ.*, **25**, 821–835.

Postma, F.M. and Ågren, J. (2016) Early life stages contribute strongly to local adaptation in *Arabidopsis thaliana*. *Proc. Natl. Acad. Sci.*, **113**, 7590–7595.

Pracharoenwattana, I., Zhou, W., Keech, O., Francisco, P.B., Udomchalothorn, T., Tschoep, H., Stitt, M., Gibon, Y. and Smith, S.M. (2010) Arabidopsis has a cytosolic fumarase required for the massive allocation of photosynthate into fumaric acid and for rapid plant growth on high nitrogen. *Plant J.*, **62**, 785–795.

Schindelin, J., Arganda-Carreras, I., Frise, E., et al. (2012) Fiji: an open-source platform for biological-image analysis. *Nat. Methods*, **9**, 676–682.

Sieger, S.M., Kristensen, B.K., Robson, C.A., Amirsadeghi, S., Eng, E.W.Y., Abdel-Mesih, A., Møller, I.M. and Vanlerberghe, G.C. (2005) The role of alternative oxidase in modulating carbon use efficiency and growth during macronutrient stress in tobacco cells. *J. Exp. Bot.*, **56**, 1499–1515.

Siloto, R.M.P., Findlay, K., Lopez-villalobos, A., Yeung, E.C., Nykiforuk, C.L. and Moloney, M.M. (2006) The accumulation of oleosins determines the size of seed oilbodies in Arabidopsis. *Plant Cell*, **18**, 1961–1974.

Silva, A.T., Ligterink, W. and Hilhorst, H.W.M. (2017) Metabolite profiling and associated gene expression reveal two metabolic shifts during the seed-to-seedling transition in *Arabidopsis thaliana*. *Plant Mol. Biol.*, **95**, 481–496.

Sweetlove, L.J., Beard, K.F.M., Nunes-Nesi, A., Fernie, A.R. and Ratcliffe, R.G. (2010) Not just a circle: flux modes in the plant TCA cycle. *Trends Plant Sci.*, **15**, 462–470.

Tcherkez, G., Gauthier, P., Buckley, T.N., et al. (2017) Tracking the origins of the Kok effect, 70 years after its discovery. *New Phytol.*, **214**, 506–510.

Tetteroo, F.A.A., Hoekstra, F.A. and Karssen, C.M. (1994) Effect of abscisic acid and slow drying on soluble carbohydrate content in developing embryoids of carrot (*Daucus carota* L.) and alfalfa (*Medicago sativa* L.). *Seed Sci. Res.*, **4**, 203–210.

Theurey, P. and Pizzo, P. (2018) The aging mitochondria. *Genes (Basel).*, **9**, 22.

Thomas, H. (2002) Ageing in plants. *Mech. Ageing Dev.*, **123**, 747–753.

Tolleter, D., Chochois, V., Poiré, R., Dean Price, G. and Badger, M.R. (2017) Measuring CO_2 and HCO_3^- permeabilities of isolated chloroplasts using a MIMS-^{18}O approach. *J. Exp. Bot.*, **68**, 3915–3924.

Üstün, S., Hafrén, A. and Hofius, D. (2017) Autophagy as a mediator of life and death in plants. *Curr. Opin. Plant Biol.*, **40**, 122–130.

Vanlerberghe, G. (2013) Alternative oxidase: a mitochondrial respiratory pathway to maintain metabolic and signaling homeostasis during abiotic and biotic stress in plants. *Int. J. Mol. Sci.*, **14**, 6805–6847.

Vidal, E.A., Moyano, T.C., Canales, J. and Gutiérrez, R.A. (2014) Nitrogen control of developmental phase transitions in *Arabidopsis thaliana*. *J. Exp. Bot.*, **65**, 5611–5618.

Vidi, P.A., Kanwischer, M., Baginsky, S., Austin, J.R., Csucs, G., Dörmann, P., Kessler, F. and Bréhélin, C. (2006) Tocopherol cyclase (VTE1) localization and vitamin E accumulation in chloroplast plastoglobule lipoprotein particles. *J. Biol. Chem.*, **281**, 11225–11234.

Vijayraghavan, V. and Soole, K. (2010) Effect of short-and long-term phosphate stress on the non-phosphorylating pathway of mitochondrial electron transport in *Arabidopsis thaliana*. *Funct. Plant Biol.*, **37**, 455–466.

Warpeha, K.M. and Montgomery, B.L. (2016) Light and hormone interactions in the seed-to-seedling transition. *Environ. Exp. Bot.*, **121**, 56–65.

Wijk, K.J. van and Kessler, F. (2017) Plastoglobuli: plastid microcompartments with integrated functions in metabolism, plastid developmental transitions, and environmental adaptation. *Annu. Rev. Plant Biol.*, **68**, 253–289.

Woo, H.R., Kim, H.J., Nam, H.G. and Lim, P.O. (2013) Plant leaf senescence and death - regulation by multiple layers of control and implications for aging in general. *J. Cell Sci.*, **126**, 4823–4833.

Wu, S.-H. (2014) Gene expression regulation in photomorphogenesis from the perspective of the central dogma. *Annu. Rev. Plant Biol.*, **65**, 311–333.

Yang, Y., Yu, X., Song, L. and An, C. (2011) ABI4 activates DGAT1 expression in Arabidopsis seedlings during nitrogen deficiency. *Plant Physiol.*, **156**, 873–883.

Yoshida, K., Terashima, I. and Noguchi, K. (2007) Up-regulation of mitochondrial alternative oxidase concomitant with chloroplast over-reduction by excess light. *Plant Cell Physiol.*, **48**, 606–614.

Zabaleta, E., Martin, M.V. and Braun, H.P. (2012) A basal carbon concentrating mechanism in plants? *Plant Sci.*, **187**, 97–104.

Zell, M.B., Fahnenstich, H., Maier, A., et al. (2010) Analysis of Arabidopsis with highly reduced levels of malate and fumarate sheds light on the role of these organic acids as storage carbon molecules. *Plant Physiol.*, **152**, 1251–1262.

Zheng, Z.-L. (2009) Carbon and nitrogen nutrient balance signaling in plants. *Plant Signal. Behav.*, **4**, 584–591.

Figure legends:

Figure 1. Developmental arrest and physiological responses to mineral starvation. (a) Morphology of liquid-grown seedlings during the four weeks of culture. Five representative seedlings are shown for each time point (numbers correspond to days of culture). The upper panel shows magnification of the apex. Black scale (2 mm), white scale (5 mm). (b) Evolution of fresh and dry weight of seedlings. Fresh weight (open circles) and dry weight (closed circles) were measured for dry seeds and seedlings collected by filtration during culture. Bars indicate SD of the mean (n = 6). (c) Evolution of dark respiration and net photosynthesis during seedling culture. Respiratory oxygen consumption (open circle) and net photosynthesis measured at 700 (closed circle) or 150 µmol photons.m^{-2}.s^{-1} (closed square) were measured by oxygraphy. Bars indicate SD of the mean (n = 3). Time 0 corresponds to the respiration measured for dry seeds imbibed for 20 minutes in the electrode.

Figure 2. Light response of net photosynthesis of Arabidopsis seedlings and mature leaves. The graph shows representative experiments of oxygen evolution by seven-day-old seedlings and four-week-old Arabidopsis leaves at different light regimes. Solid linear regression fits to the closed circles, below the break point (slope B), and dashed linear regression fits to the

open circles above the break point (slope A). Detailed values and statistical analysis are indicated in Supporting Information Table S1.

Figure 3. AOX capacity and immunodetection of AOX and GDC-H in mature leaves and seedlings. (a) Evolution of cytochrome oxidase (COX) pathway (closed circle) and AOX pathway (open circle) capacities estimated from the rates of 0.5 mM KCN sensitive or resistant oxygen consumption, respectively. Time 0 corresponds to the respiration measured in dry seeds imbibed for 20 minutes in the oxygen electrode. Bars indicate SD of the mean (n = 3). (b) Representative immunoblots of AOX and GDC-H proteins in seedlings and leaf tissue. Immunodetection was performed with anti-AOX1/2 or anti-GDC-H antibodies, and protein loading on the membrane was estimated by UV detection of Rubisco large subunit (RbcL) using Stain Free technology (Biorad). L, leaves; S, seedlings, with age in days. (c) Semi-quantitative analysis of the abundance of AOX and GDC-H proteins in each sample. On each membrane, chemiluminescence intensities in each lane were normalized to the corresponding RbcL intensity detected by UV. Data are expressed as the percentage of normalized pixels in each lane (mean ± SD) compared to d28 sample of each membrane. Letters correspond to statistically different groups according to ANOVA and Tukey's test ($p<0.05$ and $4<n<12$).

Figure 4. Analysis of soluble metabolites in dry seeds, seedlings and leaves. Metabolites were extracted and quantified from dry seeds (DS), or seedlings (d4 to d28, days of culture) and leaves (L) from four-week-old plants, collected at midday. Data correspond to the mean of three biological replicates. (a) Total amounts of sugars (white), organic acids (grey) and amino acids (black). Letters above bars correspond to statistically different groups according to ANOVA and Tukey's test ($p<0.05$). (b) Proportions of organic acids. (c) Proportion of

amino acids. The compounds (Met, Cys, Arg, Tyr, Trp, Pro, Lys) which represented less than 2.5 % of total amino acids in all samples are summed as "others".

Figure 5. Lipid droplets and fatty acid content during seedling growth and developmental arrest. (a) Visualization of lipid droplets (LDs) in seedlings using Nile red staining. At different times of culture (days), seedlings were stained with Nile red and observed by laser scanning confocal microscopy. Representative images of the upper part of seedlings are shown on the left, with views of cotyledons at a higher magnification on the right. The fluorescence of Nile red in LDs is false coloured in yellow, and chloroplast autofluorescence is shown in red. Black scale bar, 200 µm; white scale bar, 50 µm. (b) Total fatty acid content. (c) Changes in linolenic (C18:3) and eicosanoic acid (C20:1) during seedling culture (relative to total fatty acid mass). (d) Seedling content of major fatty acids. Bars indicate SD of the mean (n = 3).

Figure 6. Ultrastructural analysis of chloroplast during seedling culture. Seedlings were collected at different time points (days) and prepared for observation by transmission electron microscopy. (a) Representative micrographs of chloroplasts from cotyledon mesophyll tissue. Black scale bar, 0.5 µm; pg, plastoglobule; st, starch granule. (b) Evolution of plastoglobule surface (µm²) estimated by image analysis. Bars indicate SE of the mean ($95 < n < 138$). (c) Evolution of the frequency of plastoglobule surface values.

Figure 7. Metabolic adaptations of seedlings maintained under severe mineral starvation. The scheme highlights the main metabolic pathways contributing to energy dissipation (AOX pathway, photorespiration) and recycling of NH_3, and possibly CO_2, that occurs in the light for seedlings arrested in their development because of nutrient limitation. It also shows that photosynthates storage occurs mainly as lipids in plastoglobuli and malate in the vacuole. Dotted lines correspond to gas fluxes (CO_2, blue; O_2, red; NH_3, brown) and dashed green line

to the malate valve. AOX, alternative oxidase pathway; BC cycle, Benson and Calvin cycle; COX, cytochrome oxidase pathway; GDC/SHMT, glycine decarboxylase complex-serine hydroxymethyltransferase; GS/GOGAT, glutamine synthetase/glutamine oxoglutarate aminotransferase; Rubisco, ribulose bis-phosphate carboxylase oxygenase; TAG, triacylglycerol; TCA cycle, tricarboxylic acid cycle.

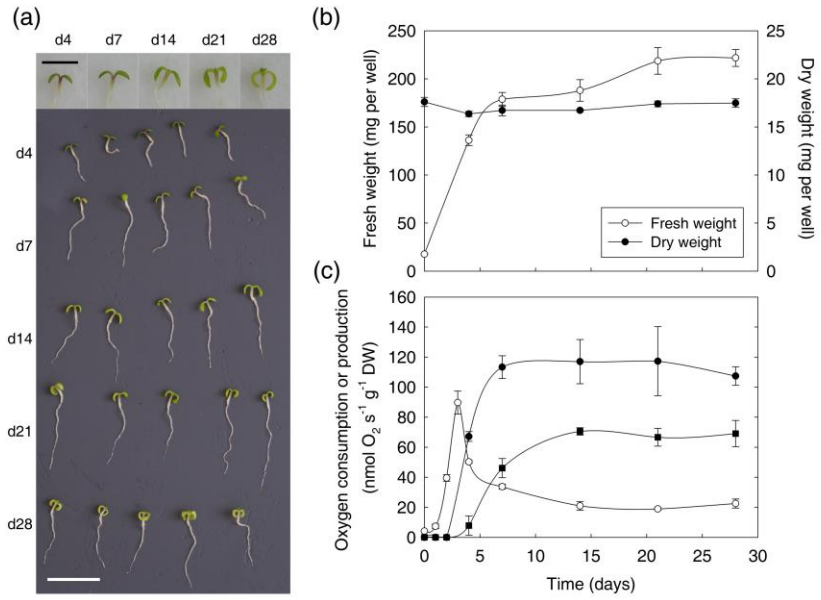

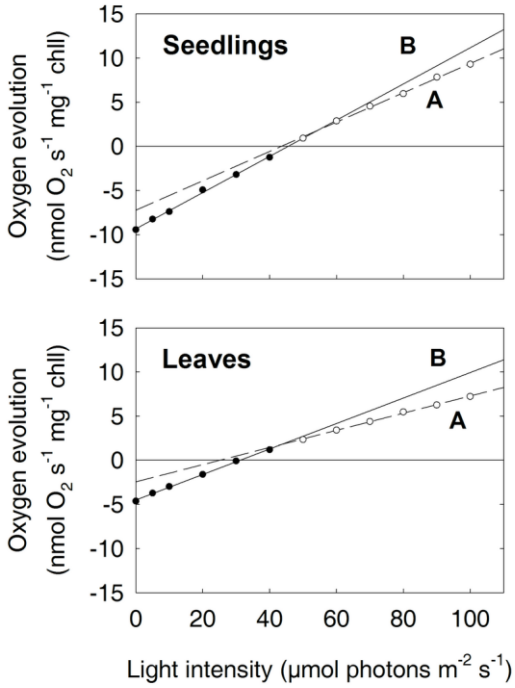

(a)

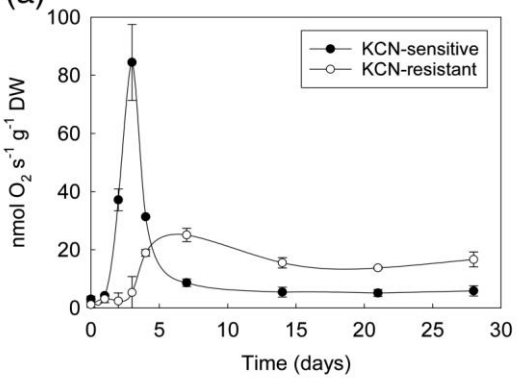

(b)

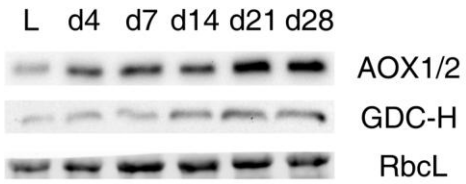

(c)

Sample	AOX	group	GDC-H	group
leaves	6.2 ± 5.5	c	27.8 ± 9.7	c
d4	40.0 ± 20.6	b	34.4 ± 14.6	c
d7	36.1 ± 16.9	b	30.1 ± 16.4	c
d14	40.2 ± 20.4	b	63.5 ± 14.3	b
d21	84.8 ± 34.8	a	107.9 ± 18.4	a
d28	100 ± 0	a	100.0 ± 0.0	a